PERFORMANCE OF GEOSYNTHETIC REINFORCED SLOPES AT FAILURE

By Jorge G. Zornberg,[1] Nicholas Sitar,[2] Members, ASCE, and James K. Mitchell,[3] Honorary Member, ASCE

ABSTRACT: A centrifuge testing program was undertaken to investigate the failure mechanisms of geosynthetic reinforced soil slopes and to evaluate the assumptions in their design. Scaling laws were established so that factors of safety in the models would be identical to those in prototype structures. Failure of the models was characterized by well-defined shear surfaces through the toe of the slopes, which is in good agreement with current design methods for reinforced slopes based on limit equilibrium. The moment of failure was defined by a sudden change in the rate of settlements at the crest of the slope. In contrast to the assumption in current design procedures that failure should initiate at the toe of a reinforced slope, failure initiated at midheight of the slopes. Model deformations were found to depend on the backfill properties, but were essentially independent of the tensile strength and spacing of the reinforcements. The test results showed that overlapping reinforcement layers contribute to stability as they failed by breakage instead of by pullout when intersected by the failure surfaces. The experimental results also indicate that stability of the reinforced slopes is governed by the peak shear strength and not by the critical state shear strength of the backfill soil. A new distribution of maximum reinforcement forces with depth, which is consistent with the failure mechanism observed in the models, is proposed for geosynthetic reinforced soil slopes.

INTRODUCTION

Conventional design of geosynthetic reinforced soil slopes is based on a limit equilibrium approach, which assumes a condition of failure. The accuracy of the limit equilibrium analysis depends on whether or not the assumed mode of failure adequately represents the conditions actually leading to collapse. Thus, observations of failures and back analyses are essential to substantiate the assumptions used in the design. However, to date, limit equilibrium predictions of the performance of geosynthetic reinforced slopes have not been fully validated against monitored failures. One consequence of this is a perceived overconservatism in design.

Small-scale physical modeling of engineered earth structures has been used in the past to provide insight into failure mechanisms in reinforced soil structures [e.g., Lee et al. (1973); Juran and Christopher (1989)]. However, a limitation of scaled physical models under 1-g conditions is that the stress levels in the models are much smaller than in the full-scale structures, thus leading to different soil properties and loading conditions. Finite element analyses have also been used to investigate failure mechanisms of reinforced soil structures [e.g., Hird et al. (1990); San et al. (1994)]. Standard finite element techniques are useful for analysis of structures under working stress conditions. However, modeling of failure in frictional materials requires special techniques to handle the localization of deformations, such as specific continuum formulations or the use of adaptive mesh refinement to capture slip discontinuities (Zienkiewicz and Taylor 1991).

The centrifuge provides a tool for geotechnical modeling in which prototype structures can be studied as scaled-down models while preserving the stress states required to develop the appropriate soil properties. The principle of centrifuge testing is to raise the acceleration of the scaled model in order to obtain prototype stress levels in the model. Although modeling limitations are often difficult to overcome when the purpose of the investigation is to compare the performance of model and prototype structures, many of these limitations can be taken into account when the purpose is to validate analytical tools. Thus, the combination of experimental centrifuge modeling results with analytical limit equilibrium predictions is a useful approach to investigate the performance of reinforced soil structures at failure. A review and evaluation of previous centrifuge studies on the performance of reinforced soil structures shows that (Zornberg et al. 1997a) (1) The focus of previous studies was mainly on the performance of reinforced vertical walls; and (2) limit equilibrium approaches were seldom used to predict the experimental results. Thus, the centrifuge testing program described herein was implemented to investigate the performance of geosynthetic reinforced soil slopes at failure.

As part of this investigation, a series of geotextile reinforced slope models was tested to failure in a geotechnical centrifuge. The variables considered in the study were the reinforcement vertical spacing, the reinforcement tensile strength, and the soil shear strength. The focus of this paper is on the interpretation of the failure mechanisms and on the implications of the experimental results on the design of geosynthetic reinforced slopes. The experimental results allow evaluation of the deformability of the models, of the pullout safety, and of the soil strength parameters governing stability. A description of the experimental setup and of the characteristics of the failure in the models is presented herein, but the reader is referred to Zornberg et al. (1997b) for further detail. The ability of limit equilibrium to predict the failure of the centrifuge models and, consequently, the suitability of limit equilibrium for the design of geosynthetic reinforced slopes is evaluated by Zornberg et al. (1998).

CENTRIFUGE TESTING OF REINFORCED SLOPES

The principle of centrifuge modeling is based upon the requirement of similarity between the model and the prototype. If a model of the prototype structure is built with dimensions reduced by a factor $1/N$, then an acceleration field of N times the acceleration of gravity, g, will generate stresses by self-weight in the model that are the same as those in the prototype structure. Additional scaling relationships can be determined either by analysis of governing differential equations or by dimensional analysis and the theory of models.

[1]Asst. Prof., Dept. of Civ., Envir., and Arch. Engrg., Univ. of Colorado, Boulder, CO 80309; formerly, Proj. Engr., Geo Syntec Consultants, Huntington Beach, CA 92648.

[2]Prof., Dept. of Civ. and Envir. Engrg., Univ. of California, Berkeley, CA 94720.

[3]Univ. Distinguished Prof. and Via Prof. of Civ. Engrg., Virginia Polytechnic Inst. and State Univ., Blacksburg, VA 24061-0105.

Note. Discussion open until January 1, 1999. Separate discussions should be submitted for the individual papers in this symposium. To extend the closing date one month, a written request must be filed with the ASCE Manager of Journals. The manuscript for this paper was submitted for review and possible publication on December 26, 1996. This paper is part of the ***Journal of Geotechnical and Geoenvironmental Engineering***, Vol. 124, No. 8, August, 1998. ©ASCE, ISSN 1090-0241/98/0008-0670–0683/$8.00 + $.50 per page. Paper No. 14816.

Besides predicting the performance of prototype structures, which is not a goal pursued in this work, centrifuge testing can be performed for at least two other important purposes, both of which are of interest in this study:

- The investigation of failure mechanisms, in which the centrifuge is used as a tool to induce, in a model structure, levels of stress that are comparable to those usually found in prototypes (Schofield 1980; Mitchell et al. 1988)
- The validation of predictive tools, in which the centrifuge is used to investigate the ability of numerical or analytical tools to predict the response of a small-scale model under prototype-like levels of stress (Shen et al. 1982; Liang et al. 1984)

Centrifuge testing, as any other experimental technique in geotechnical engineering, does not reproduce exactly the conditions at which soil exists in an earth structure. This is due to the nonhomogeneity and anisotropy of soil profiles, and to the limitations of the modeling tool. Factors that cause differences between the behavior of the model and the prototype include the acceleration field in the centrifuge, which is directly proportional to the radius of rotation in a centrifuge model but constant in the prototype; stress paths in the model, which may not be the same as those of a structure built sequentially in the field; boundary effects, such as friction between the model and the centrifuge box; and scale effects, caused by the relative size of sand grains between model and prototype. Fortunately, these effects can often be quantified and taken into account in the analytical tools used to evaluate the centrifuge test results.

The similitude requirements for evaluating the behavior of cohesionless reinforced slopes at failure are established herein by assuming the validity of limit equilibrium instead of considering generic scaling relationships. Specifically, similitude requirements are established so that factors of safety in the models are identical to those in prototype structures. For simplicity, the Ordinary Method of Slices (Fellenius 1936), which only satisfies equilibrium of moments for a circular failure surface, is considered in the limit equilibrium expressions stated below. The Factor of Safety (FS) is calculated as

$$\text{FS} = \frac{\sum \text{Moments resisting slope failure}}{\sum \text{Moments driving slope failure}} \tag{1}$$

For a prototype reinforced cohesionless slope, the Factor of Safety FS_p can be estimated in terms of the forces shown in Fig. 1 as

$$FS_p = \frac{\sum (A_i \cdot \rho \cdot g)\cos\theta_i \tan\phi\, R + \sum T_j y_j}{\sum (A_i \cdot \rho \cdot g)\sin\theta_i\, R} \tag{2}$$

where $(A_i \cdot \rho \cdot g)$ = weight of slice i per unit length of slope; A_i = area of slice i; ρ = soil density; g = acceleration due to gravity; θ_i = angle from horizontal to tangent at center of slice i; R = radius of the failure circle; ϕ = soil friction angle; T_j = tensile strength of reinforcement j; and y_j = moment arm for reinforcement j.

A similar expression can be written for the Factor of Safety FS_m of the reinforced slope model:

$$FS_m = \frac{\sum (A_{im} \cdot \rho_m \cdot g_m)\cos\theta_i \tan\phi_m R_m + \sum T_{jm} y_{jm}}{\sum (A_{im} \cdot \rho_m \cdot g_m)\sin\theta_i R_m} \tag{3}$$

where the variables with subscript m refer to the model. Variables with no subscript [e.g., in (2) and in the following equations] refer to the prototype. The following relationships exist between the model and prototype quantities:

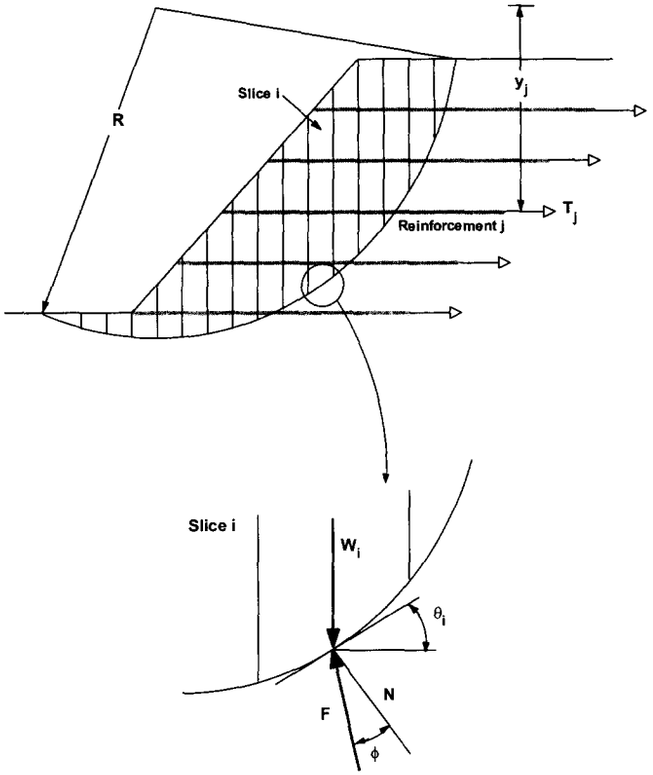

FIG. 1. Limit Equilibrium of Reinforced Soil Slope Using Circular Failure Surface

$$A_{im} = (\alpha_L)^2 \cdot A_i \tag{4}$$

$$g_m = \alpha_g \cdot g \tag{5}$$

$$R_m = \alpha_L \cdot R \tag{6}$$

$$y_{jm} = \alpha_L \cdot y_j \tag{7}$$

where α_L = scale factor for the linear dimensions; and α_g = scale factor for acceleration.

Note that a model built with a scale $\alpha_L = 1/N$ requires that the acceleration caused by gravity be scaled by $\alpha_g = N$ in order to bring the model to prototype stress levels. Incorporating (4), (5), (6), and (7) into (3), the Factor of Safety for the model can be given as

$$FS_m = \frac{\sum (A_i \cdot \rho_m \cdot g)\cos\theta_i \tan\theta_m\, R + \sum \left[\frac{T_{jm}}{(\alpha_L)^2 \alpha_g}\right] y_j}{\sum (A_i \cdot \rho_m \cdot g)\sin\theta_i\, R} \tag{8}$$

Since similarity between the failure responses of model and prototype requires that

$$FS_m = FS_p \tag{9}$$

the scaling relationships for the analysis of cohesionless reinforced slopes can then be established by comparing (2) and (8). This comparison shows that the following similitude requirements should be satisfied:

$$\rho_m = \rho \tag{10}$$

$$\tan\phi_m = \tan\phi \tag{11}$$

$$T_{jm} = (\alpha_L)^2 \alpha_g T_j = (1/N)^2 N\, T_j = (1/N) T_j \tag{12}$$

Scaling requirements (10) and (11) establish that same soil density and soil friction angle should be used in model and prototype. They can be satisfied by building the model using the same backfill soil used in the prototype structure. Condi-

tion (12) requires that the scaling factor for the reinforcement tensile strength be equal to $1/N$. That is, an Nth-scale reinforced slope model should be built using a planar reinforcement having $1/N$ the strength of the prototype reinforcement elements. Additional scale factors can be established for material parameters governing the deformability of the reinforced soil structure (Zornberg et al. 1997a). Besides establishing the scaling requirements, expressions (10), (11), and (12) identify relevant variables (density and shear strength of the soil, and layout and tensile strength of the reinforcements) for a centrifuge testing program aimed at evaluating the performance of reinforced soil slopes at failure.

SCOPE OF TESTING PROGRAM

As one of the main objectives of this study is the evaluation of design methods for geosynthetic reinforced slopes, the variables in the study were selected so that they could be taken into account within a limit equilibrium analysis framework. Accordingly, the selected variables were

- The reinforcement vertical spacing: Four different vertical spacings were adopted.
- The soil shear strength: The same sand at two different relative densities was used.
- The reinforcement tensile strength: Two model geotextiles with different tensile strength properties were selected.

In support of the centrifuge testing study, a testing program was undertaken to evaluate the strength of the sand used as backfill material, of the geotextile reinforcements, and of the interfaces that could influence the performance of the model slopes (Zornberg et al. 1998). The model slopes were built using Monterey No. 30 sand, which is a clean, uniformly graded sand classified as SP in the Unified Soil Classification System. The reinforcements selected for construction of the model slopes were two nonwoven fabrics: Pellon Sew-In (the weaker of the two fabrics, 100% polyester, mass per unit area of 24.5 g/m^2) and Pellon Tru-Grid (the stronger of the two fabrics, 60% polyester/40% rayon, mass per unit area of 28 g/m^2). The remainder of this paper refers to the weaker model reinforcement as "Geotextile W" and to the stronger model reinforcement as "Geotextile S."

The centrifuge tests performed in this study were grouped into three test series, each aimed at investigating the effect of one variable:

- *Baseline, B-series*: performed to investigate the effect of the reinforcement vertical spacing. Centrifuge models with six, nine, 12, and 18 reinforcement layers were used in this series. Monterey No. 30 sand placed at 55% relative density was used as backfill and the Geotextile W was used as reinforcement for all the models in this series. At this relative density, the peak friction angle of the sand estimated from triaxial compression tests is 35° and the reinforcement tensile strength estimated from unconfined wide-width strip tensile tests is 0.063 kN/m.
- *Denser soil, D-series*: performed to investigate the effect of the soil shear strength. A denser backfill (Monterey No. 30 sand placed at 75% relative density) than in the B-series was used for the models in this series. At this higher relative density, the peak friction angle of the sand estimated from triaxial compression tests was 37.5°. The model geotextile used as reinforcement was the same as in the B-series.
- *Stronger geotextile, S-series*: performed to investigate the effect of the reinforcement tensile strength. The models in this series were reinforced using the Geotextile S, which has a higher unconfined wide-width tensile strength (0.119 kN/m) than the Geotextile W used in the previous series. As in the B-series, Monterey No. 30 sand placed at 55% relative density was used as backfill material.

All models were built with the same slope inclination (1H:2V) and the same total height. Each reinforced slope model in this study was named using a letter that identifies the test series (B, D, or S), followed by a number that indicates the number of reinforcement layers used in the model. For example, model B12 corresponds to the reinforced slope model from the B-series built using 12 reinforcement layers.

CHARACTERISTICS OF CENTRIFUGE MODELS

The centrifuge tests were performed using a Schaevitz centrifuge at the University of California, Davis, designed to apply controlled centrifugal accelerations up to 175g and with a limit of 4,500 g·kg at a nominal radius of 1,000 mm. The payload of the testing package can be up to 45 kg. All reinforced slope models in the centrifuge testing program had the same geometry and were built within the same strong box. The models were subjected to a gradually increasing centrifugal acceleration until failure occurred.

The strong box used to contain the models had inside dimensions of 419 × 203 mm in plan × 300 mm in height. A transparent Plexiglas plate on one side of the box enabled side view of the models during testing. The other walls of the box were aluminum plates lined with Teflon to minimize side friction. The Plexiglas was lined with a Mylar sheet overprinted with a square grid pattern, which provided a reference frame for monitoring displacements within the backfill. To prevent scratches and to minimize side friction, a second plain Mylar sheet was used as protection. The box was sufficiently rigid to maintain plane strain conditions in the reinforced slope models.

The total height of the models was 254 mm (10 in.). Each model was a 228-mm- (9-in.-) high geotextile reinforced slope built over a 25.4-mm- (1 in.-) thick foundation layer. The slope face in all models was 1H:2V. Air-dried Monterey No. 30 sand was used both as backfill material and foundation soil. The number of reinforcement layers in the models varied from six to 18, giving reinforcement spacings from 37.5 mm (1.5 in.) to 12.5 mm (0.5 in.). All models were built using the same reinforcement length of 203 mm (8 in.). The use of comparatively long reinforcements was deliberate, as the focus of this study is on the evaluation of internal stability against breakage of the geotextile reinforcements. By selecting long enough reinforcements, external or compound failure surfaces were not expected to develop during testing. The geotextile layers were wrapped at the slope face. Green colored sand was placed along the Plexiglas side wall at each reinforcement level to facilitate visualization of the failure surfaces. Black colored sand markers were placed at a regular horizontal spacing (25 mm) to monitor lateral displacements within the backfill material.

To obtain consistent soil densities and placement conditions in the reinforced soil models, carefully controlled construction procedures were followed during model preparation. These procedures included sand pluviation through air under controlled discharge rate and discharge height to give uniform backfill relative densities of either 55 or 75%. A vacuum system was used to achieve the target backfill level. This system consisted of a calibrated metallic tube through which vacuum was applied to remove the excess of pluviated sand. A detailed description of the construction procedures of the reinforced slope models is presented elsewhere (Zornberg 1994; Zornberg et al. 1997a). After construction, the reinforced slope models were weighed and placed in the swing bucket of the centrifuge.

Six linear potentiometers were used to monitor the lateral

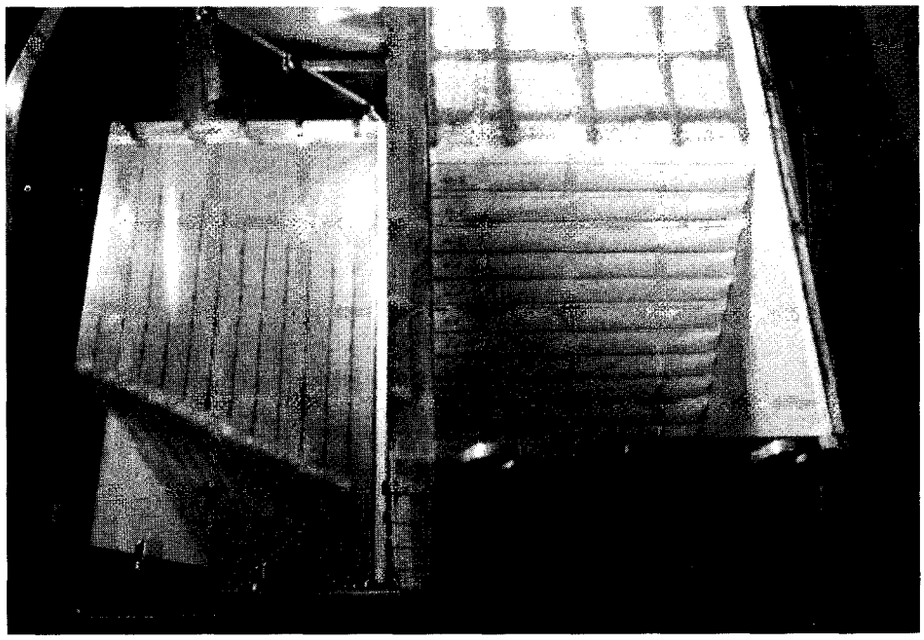

FIG. 2. Top View of Centrifuge Model, Already Placed in Swing Bucket, and Its Image through Slant Mirror

TABLE 1. Summary of Centrifuge Tests

Parameter (1)	Baseline (B-Series)				Denser Backfill (D-Series)		Stronger Geotextile (S-Series)	
	B18 (2)	B12 (3)	B9 (4)	B6 (5)	D12 (6)	D6 (7)	S9 (8)	S6 (9)
Number of reinforcement layers	18	12	9	6	12	6	9	6
Vertical spacing (mm)	12.70	19.05	25.40	38.10	19.05	38.10	25.40	38.10
Reinforcement type	Geotextile W	Geotextile W	Geotextile W	Geotextile W	Geotextile W	Geotextile W	Geotextile S	Geotextile S
Sand relative density	55%	55%	55%	55%	75%	75%	55%	55%
g-level at failure (N_f)	76.5	60	37	21	66	29	52.5	32
Failure type	Catastrophic	Catastrophic	Catastrophic	Catastrophic	Catastrophic	Catastrophic	Progressive	Progressive

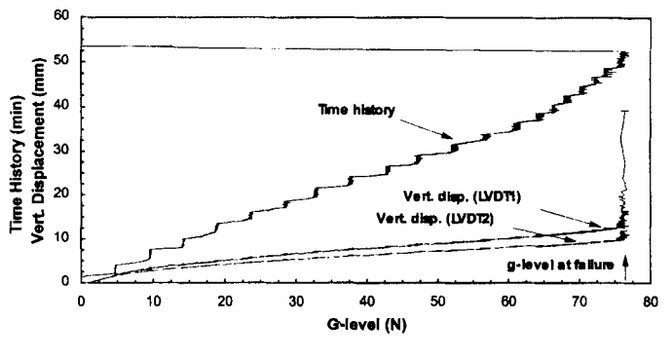

FIG. 3. Time History of Centrifugal Acceleration (N) and Settlements on Top of Model B18, Indicating Moment of Failure

displacements of the slope face. Two linear variable displacement transducers (LVDTs) were used to monitor vertical settlement at the crest of the geotextile reinforced models. A television camera, mounted at the center of the rotating structure of the centrifuge, and a video recording device were used for in-flight monitoring. A 45° mirror was used to view the model in-flight through the Plexiglas sidewall. The recorded images were used to examine the initiation of failure and to identify the failure mechanisms.

Fig. 2 shows the top view of a model already placed in the swing bucket and its image through the slant mirror. As the arm of the centrifuge spins, the bucket supported by hinged pins swings upward so that the top surface of the model is almost perpendicular to the plane of rotation. The models were subjected to a gradually increasing centrifugal acceleration until failure occurred. After failure, the models were carefully disassembled and the backfill was vacuumed out in order to retrieve the geotextile reinforcements. Inspection of the retrieved geotextiles was useful to evaluate the breakage pattern and to locate the failure surface from the observed tears.

SCOPE OF CENTRIFUGE TESTING PROGRAM

Baseline B-Series

The characteristics of the models in the B-series and the g-levels at failure obtained after centrifuge testing are presented in Table 1. All models in this series were tested using the same backfill density (55%) and the same reinforcement type (Geotextile W), but different reinforcement spacing.

Typical results obtained after centrifuge testing of one of the models from the B-series (model B18) are presented to illustrate the type of information gathered for each model throughout the study. Fig. 3 shows the history of centrifugal acceleration during testing of model B18. The acceleration was increased until failure occurred after approximately 50 min of testing when the acceleration imparted to the model was 76.5 times the acceleration of gravity. Failure development in the reinforced slope could be identified from the TV images through the Plexiglas side wall. However, settlements at the crest of the slope monitored by LVDTs proved to be invaluable to more accurately identify the moment of failure. Fig. 3 also shows the increasing settlements at the top of the reinforced slope during centrifuge testing, monitored at locations

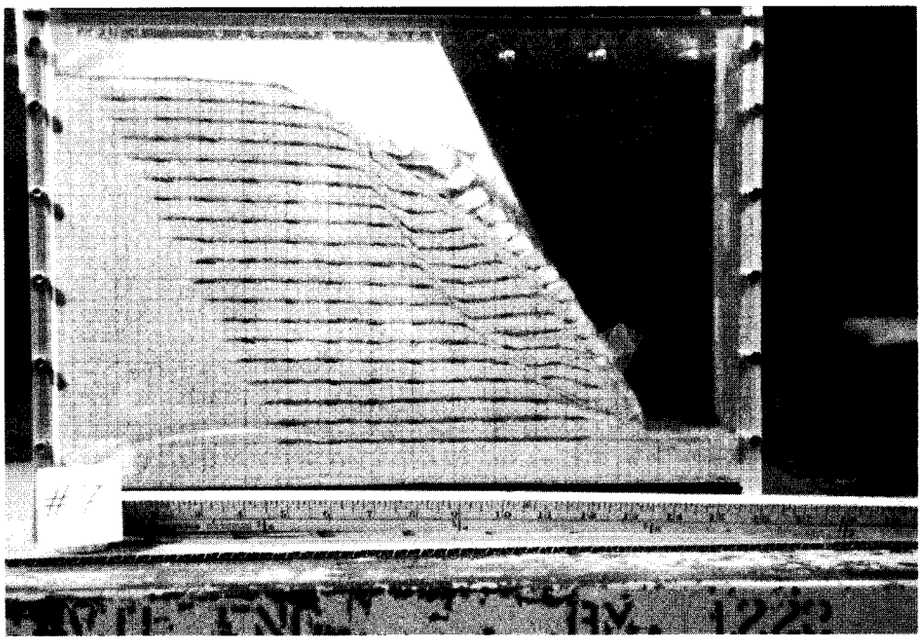

FIG. 4. View of Model B18 after Centrifuge Test

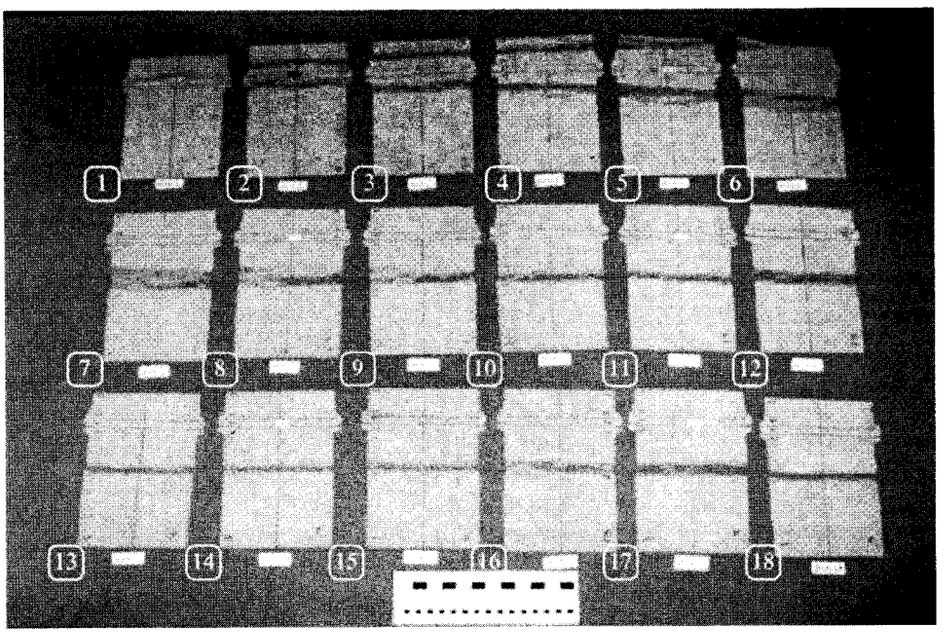

FIG. 5. Geotextile Reinforcements Retrieved from Model B18 (Numbers Indicate Reinforcement Level from Base to Top of Model)

12.5 mm (LVDT1) and 63.5 mm (LVDT2) from the crest of the slope. The sudden increase in the monitored settlements indicates the moment of failure, when the reinforced active wedge slid along the failure surface.

Recorded images showing failure development of the models were an effective way of identifying the actual shape of the failure surface and the possible failure mechanisms. Fig. 4 shows the failure surface that developed in model B18, as observed after unloading the model from the centrifuge bucket. The picture shows that the failure surface was clearly defined and went through the toe of the reinforced slope.

Following the experiment, the model was carefully disassembled in order to examine the breakage pattern in the model geotextile layers. Fig. 5 shows the 18 model geotextiles retrieved after centrifuge testing of model B18. The model geotextile shown at the top left corner of the figure (layer 1) is the reinforcement layer retrieved from the base of the reinforced slope model. The model geotextile at the bottom right corner (layer 18) is the reinforcement retrieved from the top of the model. All retrieved reinforcements show clear breaks at the location of the failure surface, indicating that internal failure occurred when the reinforcements ruptured in tension. The geotextile specimens located toward the base of the slope model show two breakage lines as the failure surface intersected both the primary reinforcement and the overlapping length. No evidence of pullout was observed, even in the short overlapping layers. As shown in the figure, the overlaps in model B18 that were fully intersected by the failure surface were those located from the base of the model up to layer 5, located 51 mm (2 in.) above the foundation. The overlaps were typically intersected by the failure surface up to an elevation of approximately one-fourth the slope height in all the centrifuge models.

Tears in the geotextile reinforcements were always perpendicular to the direction of loading, showing no evidence of edge effects caused by lateral friction between the model and

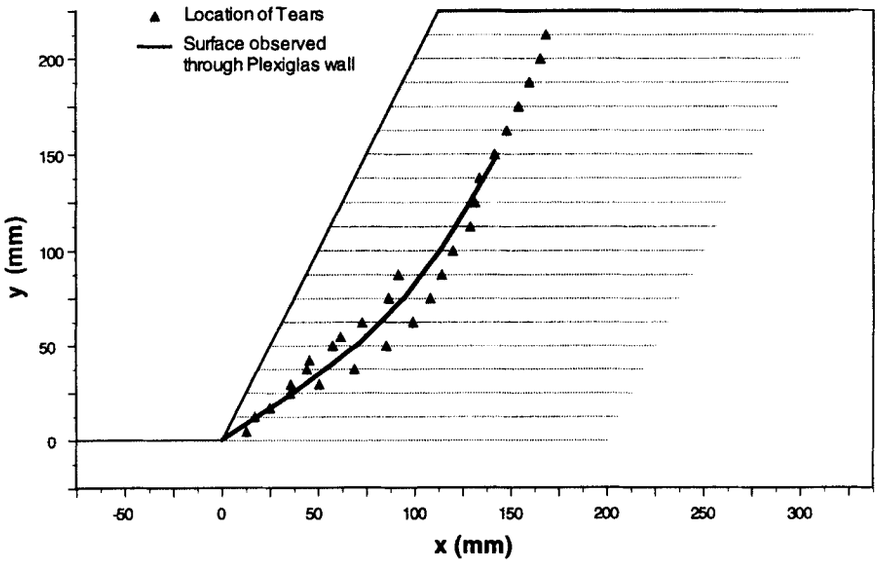

FIG. 6. Location of Failure Surface for Model B18 Obtained from Tears in Reinforcements and from In-Flight Recorded Images

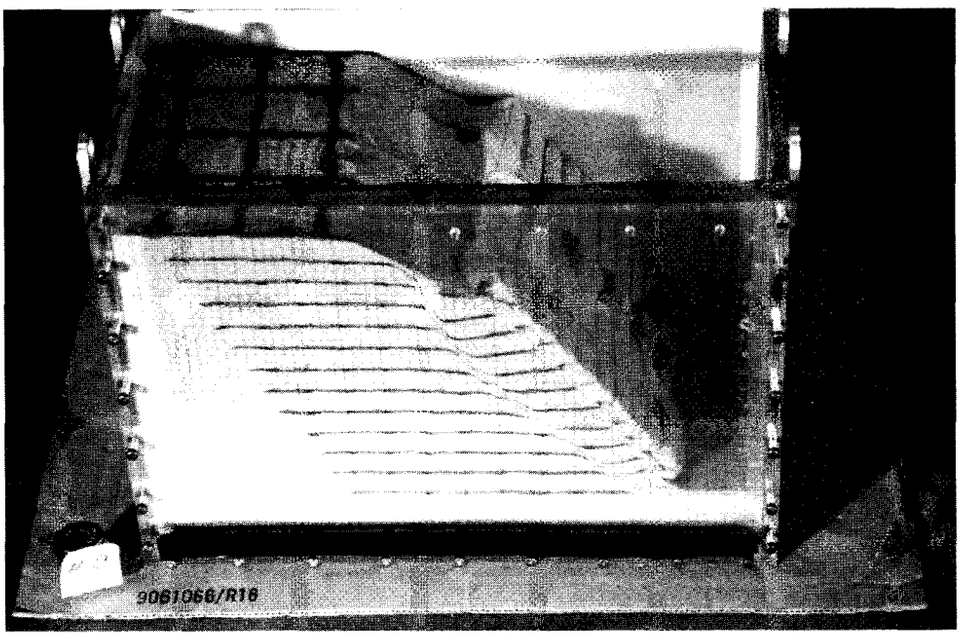

FIG. 7. Model D12 after Centrifuge Testing

the walls of the centrifuge box. If the influence of side friction had been significant, the break in the geotextile would have been curved. Additional evidence that edge effects were small was obtained by dissecting one of the models (model B6) after centrifuge testing. To preserve the model, apparent cohesion was added to the initially dry sand by wetting the backfill after centrifuge testing. Dissection of the model was then performed in order to compare the pattern of displacements observed through the Plexiglas sidewall with those at the center of the model. Displacements observed within the model and at the interface with the Plexiglas sidewall were essentially identical.

The location of the failure surface could be determined after the test by measuring the location of the tears in the retrieved geotextile primary reinforcements and overlaps. Fig. 6 shows the location of the failure surface for model B18, as measured from the tears in the retrieved model geotextiles. The failure surface caused two parallel tears instead of one clear break in some fabric specimens retrieved from model B18 (see Fig. 5). This is indicated in Fig. 6 by showing two "tear" symbols in the same layer. Fig. 6 also shows the location of the failure as digitized from the video images recorded at the moment of failure during the test. The top layers of the model were outside the range of view of the TV camera. There is good agreement between the two sets of experimental data used to estimate the location of the failure surface in the reinforced slope model. This good agreement is further evidence that edge effects during centrifuge testing were negligible. A clearly defined failure surface through the toe of the reinforced soil model was also observed in the other models from the B-series. The pattern of breakage in the geotextiles retrieved from all models in this series was similar to that observed in model B18.

Denser Soil D-Series

The characteristics of these centrifuge models, tested to failure to investigate the effect of the soil shear strength, are summarized in Table 1. Models D6 and D12 were identical to models B6 and B12, respectively, but built using Monterey No. 30 sand placed at a relative density of 75%. Fig. 7 shows

one of the models in this series, model D12, after failure. Catastrophic failure occurred after approximately 60 min of testing, when the acceleration imparted to the model was 66 times the acceleration of gravity. A clearly defined failure surface through the toe of the slope was observed in the models from the D-series. The reinforcements were also retrieved from these models after testing. As was also the case in the models in the B-series, breakage occurred in the reinforcements at the location of the failure surface, without any evidence of pullout. The overlapping layers towards the base of the slope also worked as additional reinforcements.

Stronger Geotextile S-Series

Table 1 shows the characteristics of the centrifuge models in this series, performed to investigate the effect of the reinforcement tensile strength on the stability of reinforced slopes. Models S6 and S9 corresponded to models B6 and B9 (same reinforcement layout, same sand density), but were reinforced using the Geotextile S, which has a higher tensile strength than the Geotextile W used in the B-series.

The failure surfaces that developed in the models in this series showed a wider failure zone than in the case of models built using the Geotextile W. Although models built using Geotextile S as reinforcement elements also failed along clearly defined shear surfaces, they did not exhibit the sudden collapse observed in models built using the weaker fabric. This can be explained by results of the reinforcement tensile tests, which showed that the Geotextile S undergoes comparatively larger strains after reaching the ultimate tensile strength (i.e., the maximum or peak tensile stress).

The geotextile reinforcements retrieved after testing from the models in this series showed severe straining at the location of the failure surface. However, complete separation breakage did not occur. Nevertheless, the tears and the magnitude of the localized permanent deformations in the geotextiles indicate that the reinforcements did reach their ultimate strength. As in the previous series, no evidence of pullout was observed and the overlaps near the base of the models worked as additional reinforcements.

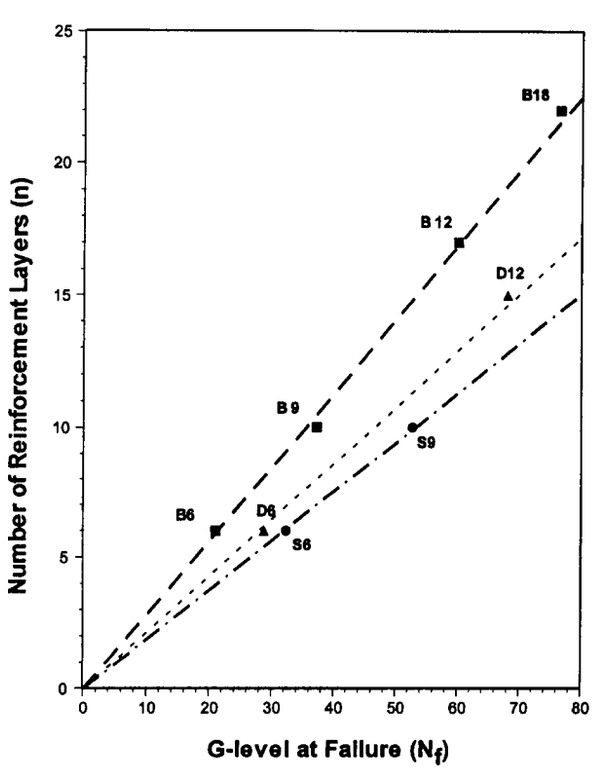

FIG. 8. G-Level at Failure for Centrifuge Models

EVALUATION OF FAILURE OF CENTRIFUGE MODELS

Measured *g*-Levels at Failure

The effect of reinforcement spacing on the stability of the reinforced slope models, as indicated by the measured *g*-level at failure N_f, is shown in Fig. 8. The number of reinforcement layers n in the figure includes the total number of model geotextiles intersected by the failure surface (i.e., primary reinforcements and overlaps intersected by the failure surface). As already stated, the overlaps intersected by the failure surface developed tensile forces and eventually failed by breakage and not by pullout. The figure shows that a clear linear relationship can be established between the number of reinforcement layers and the *g*-level at failure. As the fitted lines for each test series passes through the origin, the results in each tests series can be characterized by a single n/N_f ratio.

The n/N_f ratio for the case of the B-series equals 0.281. The effect of the soil shear strength on the stability of the centrifuge models can be assessed from the results presented in Fig. 8. The figure shows that, for a given number of reinforcement layers n, models from the Denser soil D-series failed at higher accelerations than models in the baseline B-series. The results from the centrifuge tests in the D-series define a line through the origin characterized by a ratio n/N_f of 0.215. The effect of the reinforcement tensile strength on the stability of the models can also be evaluated from the results shown in the figure. As expected, model slopes with the same number n of reinforcement layers failed at higher accelerations when reinforced with the stronger geotextile used in the S-series than when reinforced with the Geotextile W used in the B-series. The results from the centrifuge tests in the S-series define a line through the origin with a ratio n/N_f of 0.188. The rationale behind the normalization of the centrifuge test results is further discussed by Zornberg et al. (1988).

Development of Failure Surfaces

Failure of all the models in this study was characterized by the development of a well-defined shear surface approximately through the toe of the slope. The failure surfaces can be fitted using either circular, logarithmic spiral, or bilinear surfaces, which are commonly used in limit equilibrium analyses of reinforced slopes. The moment of failure was defined by a sudden change in the rate of settlements at the crest of the slope. This moment of failure agreed very well with the visual observation of the initiation of failure through the Plexiglas sidewall.

Some differences in the development of failure were observed in the different test series. In the B-series, the time elapsed between the initiation of failure and the final model collapse was relatively short. After initiation of failure, collapse generally occurred without any additional increase in the *g*-level. The time elapsed between the initiation of failure and structure collapse appeared to be even shorter in the D-series tests. This may be attributed to a rapid drop in strength of the denser backfill after it reaches its peak strength. The time elapsed between initiation of failure and final structure collapse for the models built using a stronger geotextile (S-series) was greater than for the models in the other test series. Although the failure surfaces were well defined and initiation of failure could be estimated with accuracy for the models in this series, the moment of final structure collapse was more difficult to identify than in the previous series. The postfailure performance may be attributed to the large displacements that the Geotextile S is able to sustain after reaching the ultimate

tensile strength. Thus, it appears that the postfailure behavior of the slope models before the final structure collapse depends on the postpeak behavior of both the backfill soil and, mainly, of the reinforcements.

Fig. 9(a) shows the in-flight view of one of the models (model B12) at the moment of failure initiation during centrifuge testing. This image corresponds to the moment of failure defined by the transducers that monitored the settlements at the top of the model. Careful study of the figure shows that failure initiated approximately in the middle of the slope. This can be observed by kinks in the horizontal layers of colored sand placed during construction at the reinforcement levels. The kinks initially appeared at approximately the midheight of the slope, and failure then extended rapidly to the upper half of the model. In the case of the 229-mm- (9 in.-) high model B12 shown in Fig. 9(a), initiation of failure occurred at the elevation of reinforcement layer 7 located 114 mm (4.5 in.) above the foundation. The lower geotextile layers showed no evidence of kinking until the moment of ultimate structure collapse. Failure initiated at an elevation of approximately half the slope height in all the model slopes tested as part of this investigation. This indicates that the lower reinforcement layers were not first to reach their tensile strength as is implied by current design methodologies, which assume a triangular reinforcement tension distribution with depth with a maximum tension at the base of the slope. This distribution implies that a progressive failure mechanism should initiate at the toe of the reinforced slope for uniformly spaced reinforcements of equal strength, which is inconsistent with the experimental observations. Fig. 9(b) shows the final collapse of model slope B12, as recorded in-flight, which occurred without increasing the acceleration following the failure initiation.

Because internal monitoring of the reinforcement strains was not possible due to the fragility of the model geotextiles, direct observation was used to verify the location of failure initiation. To this effect, the testing progress for one of the centrifuge models (model D6) was stopped immediately after failure initiated as monitored by the displacement transducers, but before the final collapse. Analysis of the retrieved reinforcements from model D6 confirmed that failure started approximately in the middle of the slope. While reinforcements in the upper half of the model showed the development of tears, the reinforcements in the lower half of the model showed only evidence of straining at the location of the failure surface. In fact, straining was difficult to identify in the lowermost geotextile layers. An additional piece of evidence that the reinforcement force distribution is not triangular with maximum tension at the base of the slope is that the lowermost geotextile layer did not show either tears or evidence of severe straining in any of the models.

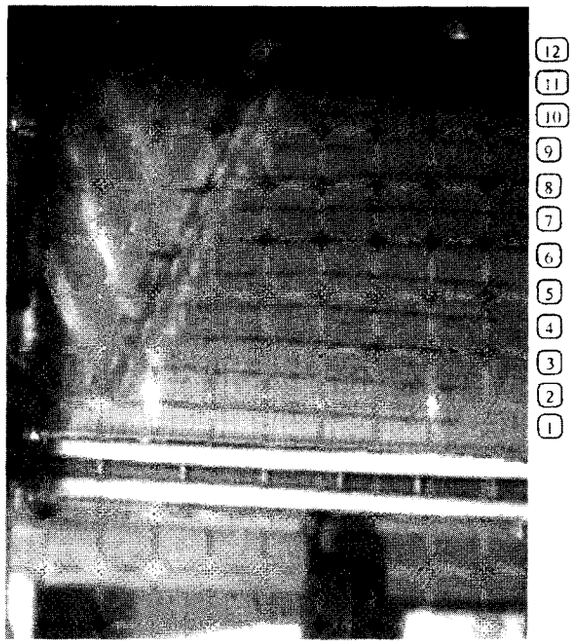

(a)

(b)

FIG. 9. In-Flight View of Model B12: (a) Failure Initiation; (b) Final Collapse

Location of Potential Failure Surfaces

The locations of the failure surfaces developed in the four models from the B-series, models B18, B12, B9, and B6, are shown in Fig. 10(a). For clarity, only the locations of the tears measured from the retrieved model geotextiles are shown in the figure. All centrifuge models appear to have failed along approximately the same failure surface, implying that location of the failure surface is independent of the vertical spacing of the reinforcement layers. This is in agreement with the results of variational limit equilibrium analyses of reinforced soil slopes by Leshchinsky and Boedeker (1989), who found that the location of the critical surfaces is independent of the reinforcement spacing. The models built using denser backfill soil (D-series) and stronger reinforcement (S-series) also failed approximately along the same failure surface.

Fig. 10(b) shows the failure surfaces for all the centrifuge models as obtained after digitizing their location from the images recorded in-flight at the moment of failure through the Plexiglas side wall. Although the images do not provide the location of the failure surface in the upper portion of the models, they show less scatter than the data obtained from measurements in the retrieved geotextiles. The results shown in the figure indicate that all centrifuge models failed along similar shear surfaces. Only model B6 developed a surface that emerged slightly above the toe of the reinforced slope model.

EVALUATION OF DEFORMATIONS

An overall discussion of the deformation of the centrifuge slope models is beyond the purposes of this study. Nevertheless, it is worth evaluating the vertical settlements measured

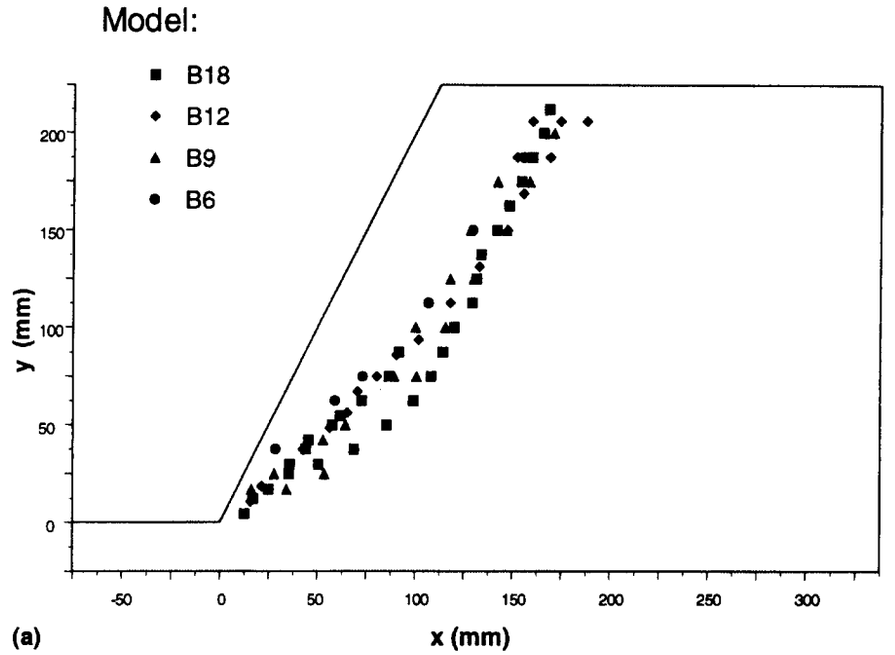

FIG. 10(a). Location of Tears in Reinforcements Models from B-Series

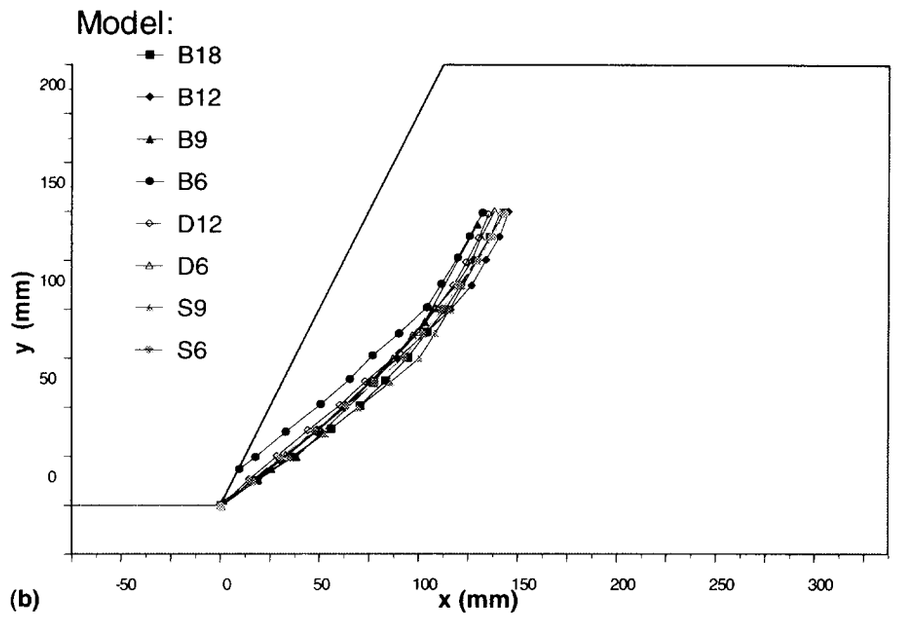

FIG. 10(b). Location of Failure Surface Obtained from In-Flight Recorded Images

at the top of the slope since they were used to determine the g-level at failure of the centrifuge tests. Fig. 11 shows the vertical settlement in several models, as monitored by the transducer located 63.5 mm from the crest of the slope. The arrows in the figure indicate the g-levels matching the initiation of failure identified by visual observation of the slope models through the Plexiglas sidewall. A similar pattern of vertical settlements was monitored by the transducer located 12.5 mm from the crest of the slope.

A noticeable feature of these data is that, for most of the models, the settlement versus g-level results appear to follow the same curve up to the moment of failure. This is the case for models S6, S9, B12, and B18, which were built with different reinforcement spacings and different reinforcement types, but with the same sand relative density. However, smaller settlements were monitored in model D6, which was built with sand placed at a higher relative density. Moreover, larger settlements were monitored in model B6, which was the model in the testing program built using the larger reinforcement spacing, the weaker reinforcement, and the looser backfill.

The effect of the difference in stress paths between model and prototypes should be evaluated before seeking a quantitative comparison between model and prototype deformations. However, the results presented herein show that deformations in slopes reinforced with extensible inclusions appear to be independent of the reinforcement spacing and of the reinforcement tensile strength. This seems to be true above a certain threshold of reinforcement spacing. Although variables such as reinforcement length were not evaluated in this testing program, the results presented herein suggest that deformations in reinforced soil slopes are not very sensitive to reinforcement characteristics and layout, but depend mainly on the properties of the backfill soil.

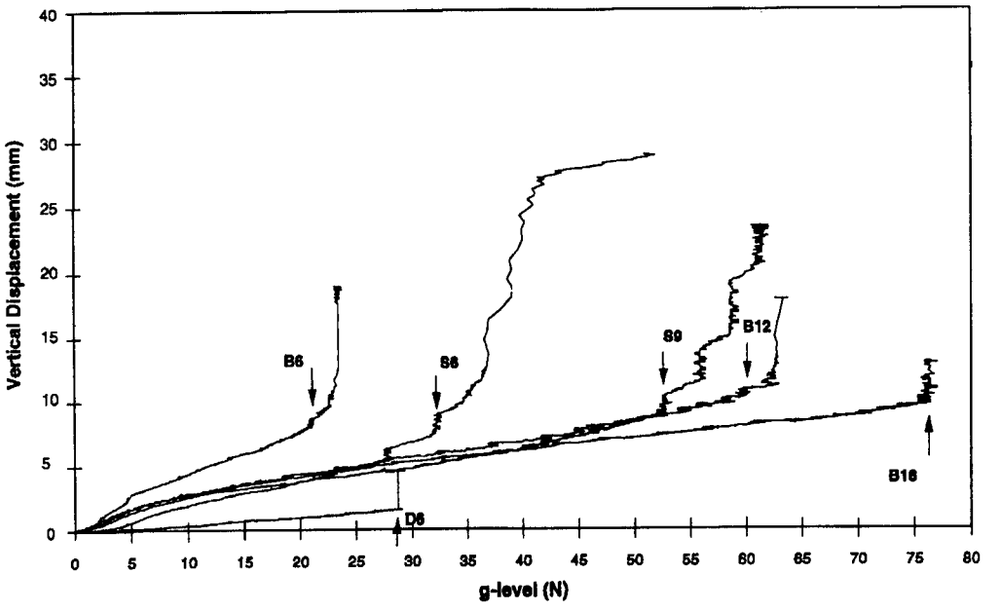

FIG. 11. Vertical Settlements on Top of Model Slopes during Centrifuge Testing (Arrows Indicate Moment of Failure in Each Test)

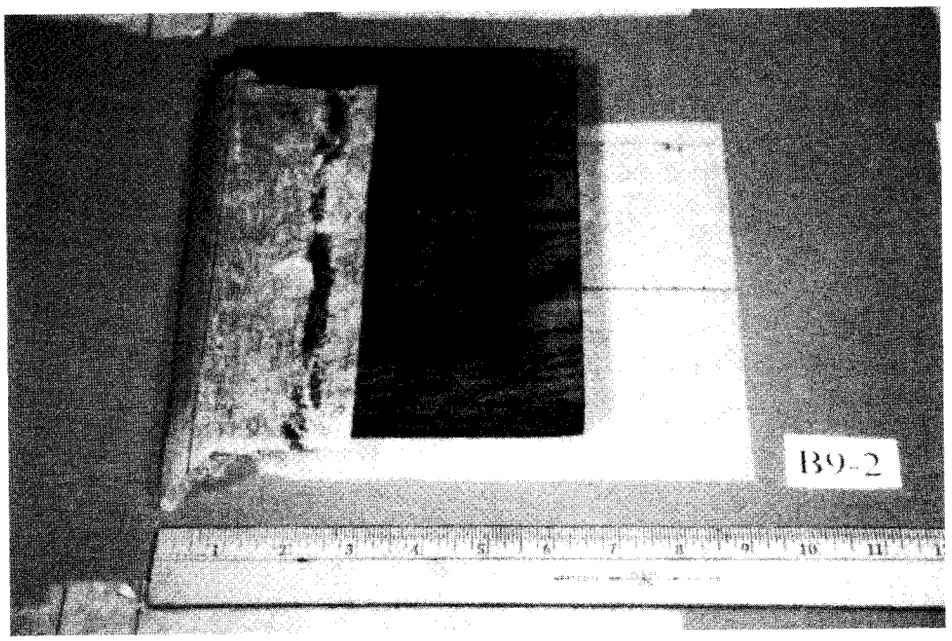

FIG. 12. Second Reinforcement Layer in Model B9, Showing Breakage in Fabric Overlap

EVALUATION OF PULLOUT SAFETY

Conventional design disregards the effect of geotextile overlaps on the stability of reinforced soil structures. However, the overlaps toward the base of the centrifuge models failed by breakage and not by pullout, indicating that this practice may be overly conservative. An evaluation using limit equilibrium analysis shows that the effect of the reinforcement overlaps in the calculated factors of safety is significant (Zornberg et al. 1998).

Sufficiently long primary reinforcements were used in the models so that they would fail by reinforcement breakage and not by pullout. However, it was somewhat unexpected to see no pullout failures in the fabric overlaps, even in cases where the anchorage length of the overlap was less than 10 mm. Nevertheless, a verification of the pullout safety of the fabric overlaps does confirm that very short overlap anchorage lengths provide sufficient pullout resistance. The pullout resistance P_r of the overlaps can be estimated as [e.g., Mitchell and Christopher (1990)]

$$P_r = 2 \cdot \sigma_v \cdot L_e \cdot \tan \delta \tag{13}$$

where σ_v = effective vertical stress; L_e = overlap length behind the failure surface; and δ = soil-reinforcement interface friction angle. Fig. 12 shows one of the fabric overlaps that was intersected by the failure surface (reinforcement layer 2 in model B9), and for which the pullout resistance is evaluated herein for illustration purposes. The anchorage length of this particular overlap is approximately 13 mm, and the vertical distance from the slope face to the fabric anchorage zone is approximately 77 mm. The pullout resistance estimated for this overlap using (13) at the moment of failure (model B9 failed at 37 g) is 0.7 kN/m. This estimated pullout resistance is considerably higher than the tensile strength of the fabric overlap. In fact, for the estimated in-soil ultimate tensile strength

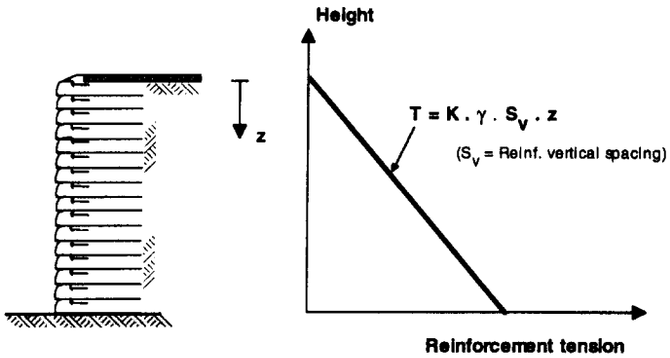

FIG. 13. Distribution with Depth of Maximum Reinforcement Tension Assumed for Design of Vertical Reinforced Soil Walls

(0.12 kN/m), enough pullout resistance would have been provided by an anchorage length as short as 2 mm.

In the absence of nonlinearity in soil shear strength, both the lateral stresses in the soil and the reinforcement pullout capacity increase linearly with centrifugal acceleration. Consequently, a model that does not fail by pullout under its own weight during construction will not do so during centrifuge testing.

EVALUATION OF SOIL SHEAR STRENGTH PARAMETERS

The criteria for characterizing reinforcements as extensible or inextensible has been established by comparing the horizontal strain in an element of reinforced backfill soil subjected to a given load, to the strain required to develop an active plastic state in an element of the same soil without reinforcement (Bonaparte and Schmertmann 1987). Accordingly, a reinforcement is classified as

- Extensible, if the tensile strain at failure in the reinforcement exceeds the horizontal extension required to develop an active plastic state in the soil
- Inextensible, if the tensile strain at failure in the reinforcement is significantly less than the horizontal extension required to develop an active plastic state in the soil

Steel reinforcements meet the criterion for inextensible reinforcements, while most currently available geosynthetic reinforcing materials meet the criterion for extensible reinforcements in almost all practical applications. The geotextiles used to reinforce the centrifuge model slopes are extensible reinforcements. Consequently, the soil strength was expected to mobilize rapidly, reaching its peak strength before the reinforcements achieve their ultimate strength. This rationale led to the recommendation, particularly by European investigators and design guidelines, to adopt the critical state soil friction angle (instead of the peak friction angle) for the design of geosynthetic reinforced slopes [e.g., McGown et al. (1989); Jewell (1991)]. However, common practice in the United States has been the use of the peak friction angle for the design of geosynthetic reinforced slopes [e.g., Christopher et al. (1990)]. It was with the purpose of clarifying this controversial issue that the same sand, placed at two different relative densities, was used as backfill material for the centrifuge models in this study.

Models in the B- and D-series were reinforced using the same geotextile reinforcement, but using sand backfill placed at two different relative densities (55 or 75%). The Monterey sand at the selected relative densities has the same soil critical state friction angle (32.5° under triaxial compression) but different peak friction angles (35° and 37.5°). As previously shown in Fig. 8, models in the D-series failed at higher g-levels than models in the B-series built with the same reinforcement spacing and reinforcement type. Since the backfill soil in models from the D- and B-series have the same critical state soil shear strength, the higher g-level at failure in the D-series models can only be attributed to the higher peak soil shear strength in these models.

The experimental results obtained in this investigation indicate that the stability of structures with extensible reinforcements is governed by the peak shear strength and not by the critical state shear strength of the backfill soil. A plausible explanation of these experimental results is that, although the soil shear strength may have been fully mobilized along certain planes in the reinforced soil mass, the maximum soil shear strength may have not been fully mobilized along the failure surface. That is, although the soil reaches an active state due to large horizontal strains compatible with the deformation of extensible reinforcements, it is feasible that large shear displacements (and drop from peak to critical shear strength) will not occur along the failure surface until sliding of the active reinforced wedge.

INTERPRETATION OF FAILURE MECHANISMS

Interpretation of the failure mechanisms in reinforced soil slopes depends on a correct assessment of the distribution with depth of maximum forces in the reinforcements. From this distribution, the location of the first reinforcement that achieves its ultimate tensile strength can be identified. Current design methods for reinforced soil vertical walls are based on the assumption that maximum reinforcement forces are proportional to the overburden pressure, as measured from the top of the vertical wall (Fig. 13). The rationale behind this assumption is that extensible reinforcements should resist the active earth pressure in the soil (Mitchell and Christopher 1990). Although interaction with the foundation soils has been found to affect this distribution in the lower reinforcement layers, studies have indicated that maximum tensile forces in geosynthetic reinforced vertical walls are well predicted by assuming a Rankine active condition [e.g., Allen et al. (1991); Zornberg and Mitchell (1994)].

In the case of reinforced soil slopes, which have their design based on limit equilibrium and not on working stress methodologies, a reinforcement force distribution with depth must also be assumed. Extending the rationale used for the case of reinforced soil vertical walls, a triangular distribution of maximum reinforcement tensions (increasing with depth from the crest of the slope) has been also assumed for the design of reinforced soil slopes. This distribution has been assumed, for example, in design charts for geosynthetic reinforced soil slopes that have been developed using limit equilibrium approaches (Schmertmann et al. 1987; Leshchinsky and Boedeker 1989; Jewell 1991). Federal Highway Administration design guidelines for reinforced soil slopes also recommend a reinforcement force distribution proportional to depth below the slope crest for the case of structures higher than 6 m [e.g., Christopher et al. (1990)].

However, since failure of the centrifuge models initiated at midheight of the slopes, the conventional triangular distribution of maximum reinforcement forces with depth is not supported by the experimental results obtained in this investigation. This has major implications for design because the reinforcement layout is currently defined considering that the most critical zone, in terms of reinforcement requirements, is at the base of the structure.

It is reasonable to assume that the reinforcements resist the horizontal stresses in the soil at the location of the potential failure surface. In the case of vertical reinforced soil walls, the horizontal soil stresses along the potential failure surface are

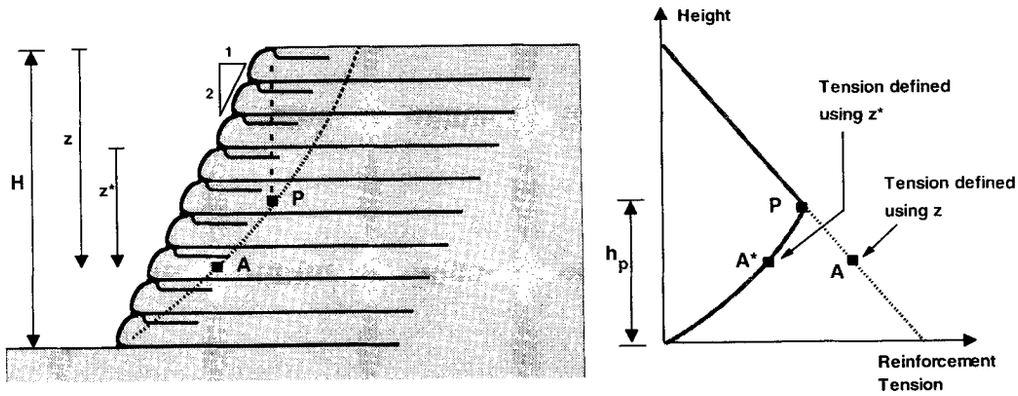

FIG. 14. Distribution with Depth of Maximum Reinforcement Tension for Reinforced Soil Slopes under Working Stresses (z and z^* Are, Respectively, Vertical Distances from Crest and from Slope Face to Generic Point A along Potential Failure Surface)

proportional to the overburden pressure which increases with depth below the top of the wall. In the case of reinforced soil slopes, horizontal soil stresses along the potential failure surface should also be proportional to the overburden pressure, which increases approximately with depth below the face of the slope. Note that the triangular distribution of reinforcement forces with depth conventionally assumed in the design of reinforced slopes stems from considering the overburden pressure to increase proportionally with depth below the crest of the slope.

A reassessment of the local equilibrium between reinforcement forces and working soil horizontal stresses provides insight into the possible reinforcement force distribution for reinforced soil slopes. Fig. 14 shows a reinforced soil slope with the two reinforcement tension distributions under discussion. The conventional triangular distribution is obtained assuming that the soil horizontal stress (and the reinforcement forces) are proportional to the overburden pressure calculated using the depth z below the crest of the slope. However, a different distribution is obtained if the soil horizontal stresses are estimated proportionally to the overburden pressure defined using the depth z^*, which is the vertical distance below the face of the slope. The two different distributions (i.e., using either z or z^*) are shown in the figure for point A along the potential failure surface. The proposed distribution is for a 1H:2V reinforced slope, which corresponds to the geometry of the centrifuge models in this study. As indicated in the figure, the location of the maximum force in the reinforcements is at a height h_P from the base of the slope. This height is determined by the location of the point P in the figure, which is the point along the potential failure surface directly below the slope crest. Above h_P, the reinforcement tension distribution increases approximately proportionally with depth below the slope crest ($z = z^*$ in this case), while below h_P the reinforcement tension decreases, being proportional to z^* and becoming zero at the toe of the slope.

In the case of a slope inclination of 1H:2V, h_P is approximately equal to one-half of the total height H of the slope. This is in agreement with the location of failure initiation in all centrifuge models in this study. Moreover, the distribution of maximum reinforcement tension with depth measured from well instrumented 1H:2V geogrid and geotextile reinforced slopes (Adib 1988; Christopher et al. 1992) appears to support the proposed distribution.

In a general case, the height h_P will depend mainly on the inclination of the face of the slope. However, the location of the maximum reinforcement force may also depend on the soil properties that may affect the location of the potential failure surface. For the case of vertical walls, the point P will be at the toe of the structure ($h_P = 0$). This is in agreement with current design methods for reinforced soil vertical walls that consider a triangular distribution of reinforcement forces with maximum tension at the base of the structure.

While Fig. 14 illustrates the distributions of reinforcement tensions under working stress conditions and helps explain the failure mechanisms in the models, substantial stress redistribution is expected to occur after the first reinforcement reaches its ultimate tensile strength, so that the distribution of reinforcement forces becomes more uniform at the moment of failure. From the results of an internally instrumented reinforced soil wall, Jaber and Mitchell (1990) noticed that stress redistribution occurred across the height of the wall before failure of the structure. In that investigation, even brittle aluminum reinforcement strips were deformable enough to redistribute the stresses across the whole height of the wall and, therefore, take advantage of the tensile strength of all reinforcement layers before failure. As the geotextiles are more ductile reinforcements elements, it is reasonable to consider that stress redistribution also occurs in geotextile reinforced slopes and that almost all reinforcements will be acting at full capacity at the moment of failure.

Fig. 15 shows the three distributions of maximum reinforcement forces that have been discussed herein. The average tension in the reinforcements T_{ave}, which is a measure of the reinforcement tension summation, is also indicated in each case. Fig. 15(a) shows the triangular reinforcement distribution that has been conventionally assumed for design of reinforced slopes. Fig. 15(b) is the estimated reinforcement tension distribution under working stresses (for a 1H:2V slope) proposed previously. The use of this maximum reinforcement force distribution with depth, limiting the maximum tension in this distribution to the reinforcement tensile strength, seems appropriate for design. The major difference between the distribution conventionally assumed in design and the one proposed herein is not the amount of reinforcement (T_{ave} is approximately the same in both cases), but the location of the critical reinforced zone. Finally, Fig. 15(c) shows the probable distribution of reinforcement forces in geosynthetic reinforced slopes approaching the moment of failure (i.e., in reinforced slopes with a stability factor of safety close to unity). At the moment of failure, the magnitude of the average tension, T_{ave}, in the reinforcements approaches the geotextile tensile strength, T_{ult}.

CONCLUSIONS

A series of geotextile reinforced soil slopes was tested in a geotechnical centrifuge in order to evaluate the performance of these structures at failure and to identify their failure mechanisms. The variables considered in the centrifuge study were the reinforcement spacing, the reinforcement tensile strength, and the soil shear strength, which can all be taken into account

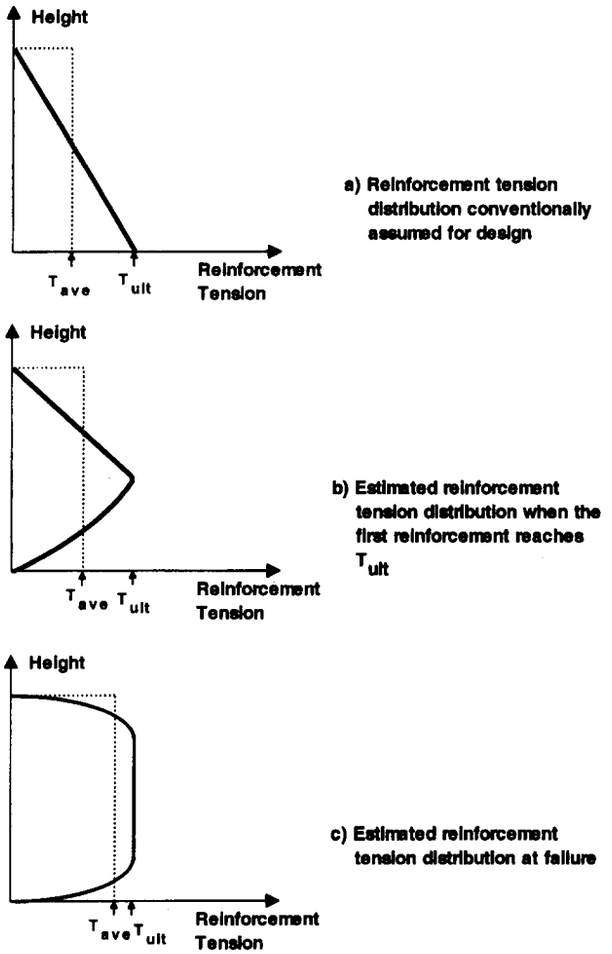

FIG. 15. Alternative Distributions with Depth of Maximum Reinforcement Tension in Reinforced Soil Slopes

using conventional limit equilibrium analyses. Scaling laws governing the problem were established in order to obtain identical factors of safety in model and prototype structures. An Nth-scale reinforced slope model should be built using planar reinforcements having $1/N$ the strength of the prototype reinforcement elements. All models were built with the same slope inclination (1H:2V) using controlled construction procedures. The moment of failure in the models was defined by a sudden change in the rate of settlements at the top of the slope, as monitored from transducers placed on the centrifuge models. The interpretation of the experimental results provided insight into the performance of reinforced slopes at failure, as follows:

- Failure in the models was characterized by well-defined shear surfaces through the toe of the slope, which is in good agreement with current design methods for reinforced slopes based on limit equilibrium.
- Failure initiated at midheight of the slopes, contradicting assumptions in current design methods that failure should develop from the toe of the reinforced slopes.
- The location of the critical failure surfaces was found to be approximately the same for all models, which were built with different reinforcement spacings, reinforcement tensile strengths, and soil densities.
- Settlements on top of the structure during centrifuge testing were observed to depend on the properties of the backfill soil, but to be essentially independent of the tensile strength and spacing of the reinforcements.
- Important contribution to the stability of the models was provided by the overlapping layers, which failed by breakage instead of by pullout when intersected by the failure surfaces.
- The test results indicate that the stability of the reinforced slopes is governed by the peak shear strength and not by the critical state shear strength of the backfill soil.
- A new distribution of reinforcement forces with depth, consistent with the failure mechanism observed in the slope models, is proposed for the design of geosynthetic reinforced soil slopes. Unlike the conventional triangular distribution of reinforcement tension with a maximum tension at the base of the slope, the location of the maximum reinforcement tension in the proposed distribution depends on the inclination of the reinforced slope. Considering the limited data in this experimental investigation, further research should be undertaken to validate the proposed distribution.

Finally, the results of this investigation show that centrifuge model testing is a useful tool to investigate the stability of earth structures, particularly in the absence of prototype failure records.

ACKNOWLEDGMENTS

Funding for this study has been provided by the California State Department of Transportation under project number RTA65T128. This assistance is gratefully acknowledged. Support received by the first writer from CNPq (National Council for Development and Research, Brazil) is also greatly appreciated.

APPENDIX I. REFERENCES

Adib, M. E. (1988). "Internal lateral earth pressure in earth walls," PhD dissertation, Dept. of Civ. Engrg., University of California, Berkeley, Calif.

Allen, T. M., Christopher, B. R., and Holtz, R. D. (1991). "Performance of a 12.6 m high geotextile wall in Seattle, Washington." *Int. Symp. on Geosynthetic-Reinforced Soil Retaining Walls*, A. A. Balkema, Rotterdam, The Netherlands, 81–100.

Bonaparte, R., and Schmertmann, G. R. (1987). "Reinforcement extensibility in reinforced soil wall design." *The application of polymeric reinforcement in soil retaining structures*, P. M. Jarrett and A. McGown, eds., Nato Advanced Research Workshop, Royal Military College of Canada, Ont., Canada, 409–457.

Christopher, B., Bonczkiewicz, C., and Holtz, R. (1992). "Design, construction and monitoring of full scale test of reinforced soil walls and slopes." *Recent case histories of permanent geosynthetic-reinforced soil retaining walls*, F. Tatsuoka and D. Leshchinsky, eds., A. A. Balkema, Tokyo, Japan, 45–60.

Christopher, B. R., et al. (1990). "Design and construction guidelines for reinforced soil structures—volume I." *Rep. No. FHWA-RD-89-043*, Federal Highway Administration, U.S. Department of Transportation, Washington, D.C.

Fellenius, W. (1936). "Calculation of the stability of earth dams." *Proc., 2nd Congr. Large Dams*, Vol. 4, Washington, D.C., 445–462.

Hird, C. C., Pyrah, I. C., and Russell, D. (1990). "Finite element analysis of the collapse of reinforced embankments on soft ground." *Géotechnique*, London, U.K., 40(4), 633–640.

Jaber, M., and Mitchell, J. K. (1990). "Behaviour of reinforced soil walls at limit state." *Performance of reinforced soil structures*, A. McGown, K. Yeo, and K. Z. Andrawes, eds., Thomas Telford Ltd., London, U.K., 53–57.

Jewell, R. A. (1991). "Application of revised design charts for steep reinforced slopes." *Geotextiles and Geomembranes*, 10, 203–233.

Juran, I., and Christopher, B. R. (1989). "Laboratory model study on geosynthetic reinforced soil retaining walls." *J. Geotech. Engrg.*, ASCE, 115(7), 905–926.

Lee, K. L., Adams, B. D., and Vagneron, J. J. (1973). "Reinforced earth retaining walls." *J. Soil Mech. and Found. Div.*, ASCE, 99(10), 745–764.

Leshchinsky, D., and Boedeker, R. H. (1989). "Geosynthetic reinforced soil structures." *J. Geotech. Engrg.*, ASCE, 115(10), 1459–1478.

Liang, R. K., Tse, E. C., Kuhn, M. R., and Mitchell, J. K. (1984). "Evaluation of a constitutive model for soft clay using the centrifuge." *Proc., Symp. on Recent Adv. in Geotech. Centrifuge Modeling*, University of California, Davis, Calif., 55–70.

McGown, A., Murray, R. T., and Jewell, R. A. (1989). "State-of-the-art report on reinforced soil." *Proc., 12th Int. Conf. Soil Mech. and Found. Engrg.*, A. A. Balkema, Rotterdam, The Netherlands, 4.
Mitchell, J. K., and Christopher, B. R. (1990). "North American practice in reinforced soil systems." *Des. and Perf. of Earth Retaining Struct., Geotech. Spec. Publ. No. 25*, ASCE, June, 322–346.
Mitchell, J. K., Jaber, M., Shen, C. K., and Hua, Z. K. (1988). "Behavior of reinforced soil walls in centrifuge model tests." *Proc., Centrifuge 88*, A. A. Balkema, Rotterdam, The Netherlands, 259–271.
San, K., Leshchinsky, D., and Matsui, T. (1994). "Geosynthetic reinforced slopes: Limit equilibrium and finite element analysis." *Soils and Found.*, Tokyo, Japan, 34(2), 79–85.
Schmertmann, G. R., Chouery-Curtis, V. E., Johnson, R. D., and Bonaparte, R. (1987). "Design charts for geogrid-reinforced soil slopes." *Proc., Geosynthetics'87 Conf.*, New Orleans, La., 108–120.
Schofield, A. (1980). "Cambridge geotechnical centrifuge operations." *Géotechnique*, 30(3), 227–268.
Shen, C., Kim, Y., Bang, S., and Mitchell, J. K. (1982). "Centrifuge modeling of lateral earth support." *J. Geotech. Engrg. Div.*, ASCE, 108(9), 1150–1164.
Zienkiewicz, O. C., and Taylor, R. L. (1991). *The finite element method*, 4th Ed., Vol. 2, McGraw-Hill Book Co. Inc., New York, N.Y.
Zornberg, J. G. (1994). "Performance of geotextile-reinforced soil structures," PhD dissertation, Dept. of Civ. Engrg., University of California, Berkeley, Calif.
Zornberg, J. G., and Mitchell, J. K. (1994). "Finite element prediction of the performance of an instrumented geotextile-reinforced wall." *Proc., 8th Int. Conf. of the Int. Assn. for Comp. Methods and Adv. in Geomechanics (IACMAG'94)*, Vol. 2, A. A. Balkema, Rotterdam, The Netherlands, 1433–1438.
Zornberg, J. G., Mitchell, J. K., and Sitar, N. (1997a). "Testing of reinforced soil slopes in a geotechnical centrifuge." *ASTM Geotech. Testing J.*, 20(4), 470–480.
Zornberg, J. G., Sitar, N., and Mitchell, J. K. (1997b). "Failure of steep reinforced soil slopes." *Proc., Geosynthetics '97 Conf.*, Vol. 1, Long Beach, Calif., 55–72.
Zornberg, J. G., Sitar, N., and Mitchell, J. K. (1998). "Limit equilibrium as basis for design of geosynthetic reinforced slopes." *J. Geotech. and Geoenvironmental Engrg.*, ASCE, 124(8), 684–698.

APPENDIX II. NOTATION

The following symbols are used in this paper:

A_i = area of slice i (m^2);
FS = factor of safety (dimensionless);
g = acceleration of gravity (m^2/s);
h_P = elevation at level of maximum reinforcement tension (m);
L_e = embedment length (m);
N = g-level imparted to centrifuge model (dimensionless);
N_f = g-level at failure (dimensionless);
n = number of reinforcement layers (dimensionless);
R = radius of failure circle (m);
T_j = tensile strength of reinforcement j (kN/m);
y_j = moment arm for reinforcement j (m);
z = depth below slope crest (m);
z^* = depth below slope face (m);
α_g = scale factor for acceleration (dimensionless);
α_L = scale factor for linear dimensions (dimensionless);
δ = interface friction angle (degrees);
θ_i = angle from horizontal to tangent at center of slice i (degrees);
ρ = soil density (kg/m^3);
σ_v = effective vertical stress (kN/m^2); and
ϕ = soil friction angle (degrees).